

FEM Estimation and Comparison of Material Properties of Thin Spherical Perforated Plate and Thin Perforated Flat Plate

Collins Juma¹ and Ihn Namgung^{2*}

¹Graduate Student, KEPCO International Nuclear Graduate School, Korea.

²Professor, KEPCO International Nuclear Graduate School, Korea.

Abstract

Perforated plates are used for the steam generator tube-sheet and the Reactor Vessel Closure Head in the Nuclear Power Plant. The structural integrity of these perforated structures is vital for the operational safety of the Nuclear Power plant. The ASME code, Section III Appendix A-8000, addresses the analysis of perforated plates when subjected to either directly applied loads or loadings resulting from structural interaction with adjacent members. However, this analysis is only limited to the flat plate with a triangular perforation pattern. This paper utilizes the ASME code concept of the equivalent material properties to extend the analysis to the spherical perforated plate. Based on the concept of the effective elastic constants, simulation of both flat and spherical perforated plates and their equivalent solid plates were carried out using Finite Element Analysis (FEA). The isotropic material properties of the perforated plate were replaced with anisotropic material properties of the equivalent solid plate and subjected to same loading and boundary conditions. The difference between the deformation of the perforated and equivalent solid plate was optimized for convergence by varying the effective elastic constants. The effective elastic constants vs ligament efficiency curves were then generated. For the flat perforated plate, the curves obtained are in agreement with the design curve provided by ASME code. Based on this finding, FEA simulation was extended to the spherical plate and a similar design curve was developed. This curve is applicable to both thick and thin plate with a triangular perforation pattern. Using this curve, the perforated spherical plate can be analyzed by their equivalent solid spherical plate.

Keywords - Perforated Flat Plate, Perforated Spherical Plate, Equivalent Elastic Constants, Equivalent Poisson's Ratio

I. INTRODUCTION

In the nuclear industry, thick perforated plates are used for the steam generator tube-sheet and the Reactor Vessel Closure Head. Design and structural analysis of the perforated plate is based on the concept of the equivalent solid plate.

The ASME Section III Appendix A-8000 [1] provides a procedure for analysis of the perforated plate based on the equivalent solid plate concept. A solid plate with modified elastic constant values and geometrically similar to the perforated plate is used to analyze a perforated plate. This analysis method is applicable to the flat perforated plate

subjected to direct loadings or loadings resulting from structural interaction with adjacent members provided the perforated plate:

- Have circular holes in an array of equilateral triangles.
- A minimum number of holes is 19.
- Have a Ligament efficiency greater than 5% ($\eta \geq 0.05$).

The Fig 1 below shows ASME design curve showing the relationship between effective elastic constants and the equivalent material properties.

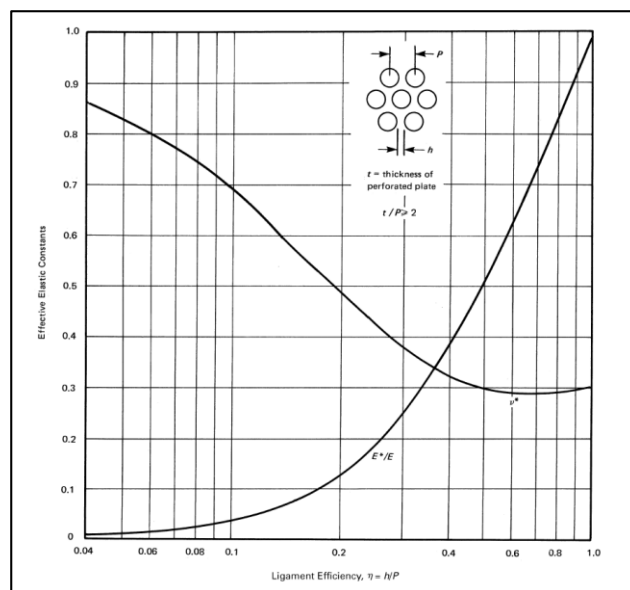


Figure 1. Equivalent material properties

Although ASME Section III Appendix A-8000 provides the procedure for determining the effective elastic constant, it is only applicable to a flat perforated plate and limited literature is available on the analysis of the spherical perforated plate.

Extensive research has been carried out on the method of determining the equivalent material properties of a perforated plate based on the equivalent solid plate concept [2, 3, 4].

Horvay, Malkin and Salerno et al. [2] had developed numerical methods based on analyzing the stress and displacements in perforated structures that were geometric approximations of the actual perforated plate with circular holes in a doubly-periodic

*Corresponding author, inamgung@kings.ac.kr

array. However, the solution obtained by these methods was limited to low ligament efficiencies.

Slot and W. J O'Donnell [4] determined the effective elastic constants for a range of ligament efficiencies and Poisson's ratio. This was based on the concept that the deformation of the perforated plate is similar to that of the equivalent solid plate subjected to similar loading conditions.

Bailey and Hicks, [4] theoretically obtained the design curve for determining the equivalent material properties. However, nonlinear equivalent material properties were not considered.

Duncan J.P and Upfold, R.W [5] adopted the equivalent solid plate concept to determine the effective elastic constant. The isotropic material properties of the perforated plate were replaced with orthotropic material properties of an equivalent solid plate subjected to the same loading conditions.

In this research, the effective elastic constants for a flat and spherical plate with a triangular perforation pattern was examined using the FEA simulation. By varying ligament efficiencies, pitch ratio, and thickness a series of FEA simulations were performed.

The ASME Section III Appendix A-8000 was then used to validate the FEA results for the flat perforated plate and to justify FEA methodology. The same concept was then extended to spherical perforated plate in order to determine the equivalent elastic constants.

II. EQUIVALENT MATERIAL PROPERTIES FOR THE FLAT PERFORATED PLATE

The effective elastic constants are determined in such a way that the gross deformation in the perforated plate and the equivalent solid plate are identical under similar loading and boundary conditions.

Equivalent material constants are used to simulate the behavior of the perforated plate as an equivalent solid plate and are obtained based on the ligament efficiency (η) as well as the ratio of plate thickness to pitch ($h(p)$). The ligament efficiency (η) is defined by (1).

$$\eta = \frac{h}{p} = \frac{p-d}{p} \quad (1)$$

Where;

h thickness of the plate.

p pitch(distance between the center of holes).

d diameter of the hole.

ASME code [1] gives equivalent elastic constants for a plane stress conditions. However, for a thick plate relative to the diameter of the perforation, generalized plane strain conditions are more realistic. Hence, the relationship between effective elastic constants for both plane stress and the generalized plane strain conditions was formulated by "Slot and O'Donnell" [4].

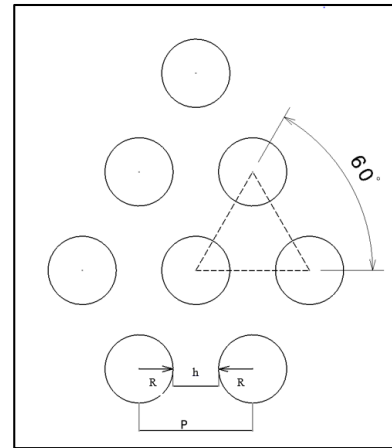


Figure 1: Plane view of the triangular perforate plate.

Based on the theory of elasticity, stresses, strain, and displacement of a perforated plate under plane stress condition are defined by:

$$E^* = \frac{\sigma^*}{\epsilon^*} \quad (2)$$

$$G^* = \frac{\tau^*}{\gamma^*} \quad (3)$$

$$\epsilon_x = \frac{\partial u}{\partial x} = \frac{(\sigma_x - \nu \sigma_y)}{E} \quad (4)$$

$$\epsilon_y = \frac{\partial v}{\partial y} = \frac{(\sigma_y - \nu \sigma_x)}{E} \quad (5)$$

$$\gamma_{xy} = \frac{\partial u}{\partial y} + \frac{\partial v}{\partial x} = \frac{\tau_{xy}}{G} \quad (6)$$

Where (*) is the equivalent properties.

The relationship between the plane stress constants and material constants can be expressed such that the Effective Young's modulus (E^*) is directly proportional to Young's modulus (E) of the perforated plate material while the effective Poisson's ratio (ν^*) is linearly dependent on the Poisson's ratio (ν) of the material [6] and this can be defined by;

$$E^* = EF(\eta) \quad (7)$$

$$\nu^* = G(\eta) + \nu F(\eta) \quad (8)$$

For a given value of ligament efficiency (η) where $F(\eta)$ and $G(\eta)$ are constants.

The function $G(\eta)$ provides a value of $\nu^* = \nu_0^*$ for $\nu = 0$ which is an intercept value.

Substituting (7) in (8)

$$\nu^* = \nu_0^* + \left(\frac{E^*}{E}\right) \nu \quad (9)$$

Effective elastic constants are obtained by superposition of strain ($\epsilon_z = 0$).

For plane strain condition, (ϵ_z is uniform).

$$E^* = \frac{G^*}{(1-\nu^2)} \quad (10)$$

$$\nu^* = \nu_0^* + \left(\frac{\nu E^*}{E(1-\nu)} \right) \quad (11)$$

$$G^* = \frac{E^*}{2(1+\nu^*)} \quad (12)$$

Where;

E^* = Effective Young's Modulus in plane stress condition.

ν^* = Effective Poisson's ratio in plane stress condition.

G^* = Effective Shear Modulus in plane stress condition.

ν_0^* = Value of ν^* when $\nu = 0.3$

Therefore equivalent solid plate stress-strain relation under plane strain condition can be given by;

$$\epsilon_x^* = \frac{\sigma_x^*}{\bar{E}^*} - \bar{\nu}^* \frac{\sigma_y^*}{\bar{E}^*} \quad (13)$$

$$\epsilon_y^* = \frac{\sigma_y^*}{\bar{E}^*} - \bar{\nu}^* \frac{\sigma_x^*}{\bar{E}^*} \quad (14)$$

$$\gamma_{xy}^* = \frac{\tau_{xy}^*}{\bar{G}^*} \quad (15)$$

Given that $G^* = \bar{G}^*$

Where;

\bar{E}^* Effective Young's Modulus in plane strain condition.

$\bar{\nu}^*$ Effective Poisson's ratio in plane strain condition.

\bar{G}^* Effective Shear Modulus in plane strain condition.

For plane strain $\epsilon_z = 0$

$$\epsilon_z = \frac{\sigma_z}{E} - \frac{\nu(\sigma_x + \sigma_y)}{E} = 0 \quad (16)$$

Where;

$$\sigma_z = (\sigma_x + \sigma_y) \quad (17)$$

Considering that the perforated plate is relatively thick in comparison with the pitch dimension, the equivalent elastic constants are determined based on the generalized plane strain condition.

$\epsilon_z = \text{uniform}$ And σ_z vanishes in a general plane strain. Therefore the effective elastic constants are obtained by superposition of strain produced under plane strain condition

and strains that results from annihilating the associated average surface traction σ_z^* [4].

$$\epsilon_x^* = \frac{\nu \sigma_z^*}{E_z^*} = \frac{\nu^2 (\sigma_x^* + \sigma_y^*)}{E_z^*} \quad (18)$$

$$\epsilon_y^* = \frac{\nu \sigma_z^*}{E_z^*} = \frac{\nu^2 (\sigma_x^* + \sigma_y^*)}{E_z^*} \quad (19)$$

$$\gamma_{xy}^* = 0 \quad (20)$$

The effective Young's modulus for the triangular penetration in the thickness direction is obtained by;

$$E_z^* = \frac{(1-\pi(1-\eta)^2)}{2\sqrt{3}} \quad (21)$$

The effective Young's modulus and the Poisson's ratio are related to the plane stress by the following equations:

$$\bar{E}^* = \left[\frac{(1-\nu^2)}{E^*} + \frac{\nu^2}{E_z^*} \right]^{-1} \quad (22)$$

$$\bar{\nu}^* = \bar{E}^* \left[\frac{(1-\nu^2)\nu_0^*}{E^*} + \frac{\nu(1+\nu)}{E} - \frac{\nu^2}{E_z^*} \right] \quad (23)$$

$$\nu^* = \nu_0^* + \left(\frac{E^*}{E} \right) \nu \quad (24)$$

Substituting ν_0^* of (24) in (23) and \bar{E}^* of (22) in (23) ,

$$\bar{\nu}^* \left(\frac{E^*}{E} \right) = \left[\nu^3 + \nu^2 \left(1 - \frac{E^*}{E_z^*} \right) + (1 - \nu^2) \nu^* \frac{E}{E^*} \right] \quad (25)$$

Where;

\bar{E}^* Effective Young's Modulus in general plane strain condition

$\bar{\nu}^*$ Effective Poisson's ratio in general plane strain condition.

III. METHODOLOGY

III.I Modeling of perforated and equivalent solid plate

In this study, the equivalent material properties for a flat perforated plate was extended to the spherical perforated plate. Using FEA, the perforated plates, both Flat and Spherical, with triangular perforation patterns and their equivalent solid plates of uniform thickness 5mm were developed. The triangular perforations pattern on the plate was defined by 39 circular holes with a radius of 9.5mm normal to the plate surface with a pitch of 20 mm as shown in Fig 2, Fig 3 and Fig 4 below.

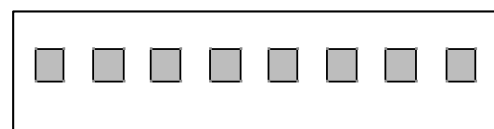


Figure 1: Flat perforated plate

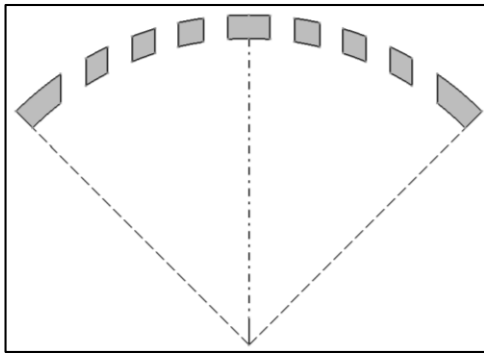


Figure 3: Perforations parallel to plane

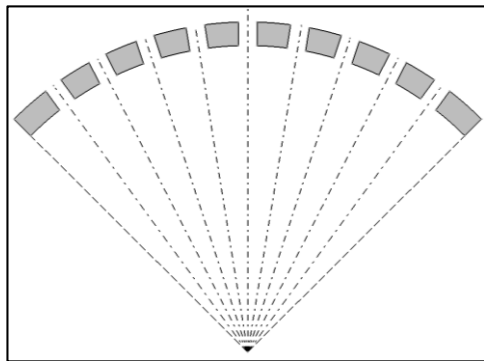


Figure 4: Perforations normal to surface

Ligament efficiencies (η) for a given range of $0.05 \leq \eta \leq 1$ [1] were computed using equation 1 by varying the diameter of the holes and the distance between the center of the holes (pitch).

III.II Loading conditions and material Definition

A pressure of magnitude 2 MPa acting normal to the solid surface area of the perforated plate in the z-direction with different ligament efficiencies was made equal to that acting normal to the surface of the equivalent solid plate. This was to ensure that both the perforated and equivalent solid plate is subjected to the similar loading condition as shown in Fig 6 and Fig 7 below.

Isotropic material properties of the perforated plates were replaced with anisotropic properties of the equivalent solid plate. Engineering constants of the perforated plates were defined as $E = 2 \times 10^{11} Pa$, $\nu = 0.3$ and $G = 7.692 \times 10^{10} Pa$.

III.III Optimization

Based on the equivalent elastic concept, the overall deformation of the equivalent solid plate is the same as that of the perforated plate when subjected to the same loading conditions Slot and W. J O'Donnell [4].

$$\delta_{Perforated\ plate} = \delta_{Equivalent\ Solid\ Plate} \quad (26)$$

From the FEA simulation, deformation on different points equally spaced on both the perforated and equivalent solid plate was determined.

Optimization for the deformation of the perforated and equivalent solid plate was carried out by varying the values of the equivalent material properties so that the summation of the difference of the absolute value for deformation convergence.

$$f(E', \nu') \equiv \delta_{Total} = 0 \quad (27)$$

$$\delta_{Total} = |u_1 - u'_1| + |u_2 - u'_2| + \dots + |u_{n+1} - u'_{n+1}| \quad (28)$$

Inevitably, considerable FEA simulation was involved for different values of ligament efficiencies for the flat and spherical perforated plate and their equivalent solid plates.

This is summarized in Fig 5 below.

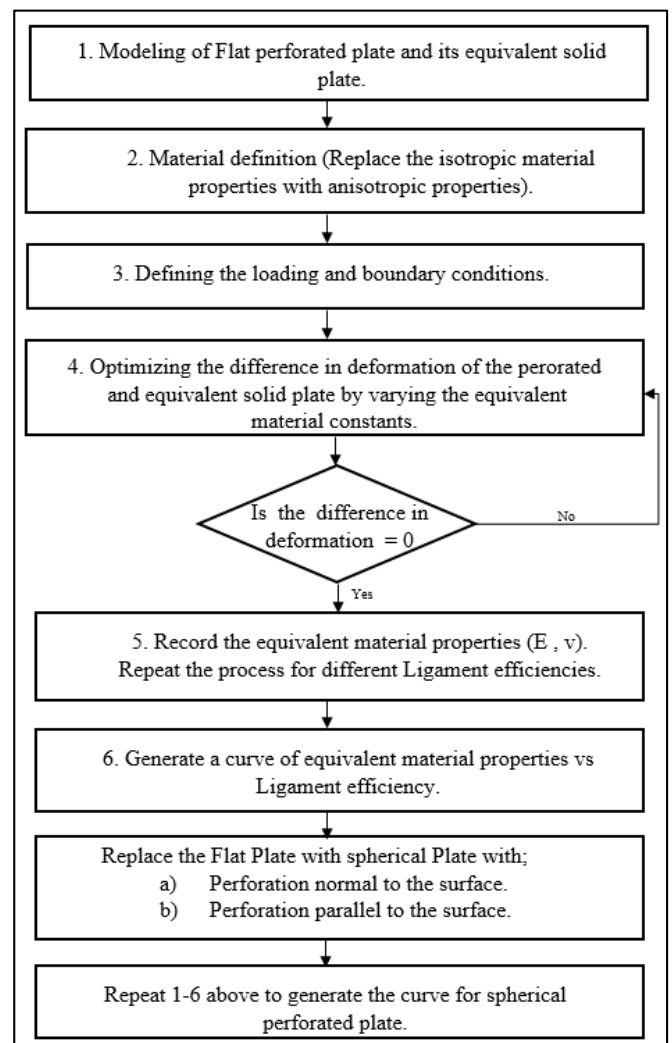


Figure 5: Procedure to determine the equivalent material constants

Fig 6 shows analysis model and boundary condition for perforated plate and solid plate. Fig 7 shows analysis model and boundary condition for perforated spherical plate and solid plate.

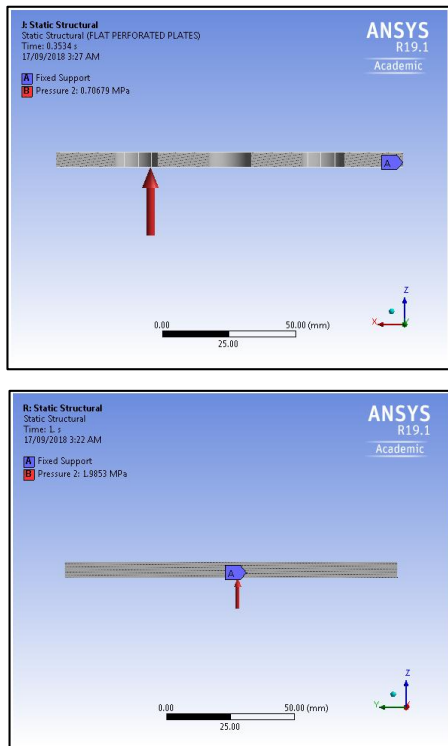


Figure 6: Flat perforated plate and equivalent solid plate loading and boundary conditions setup

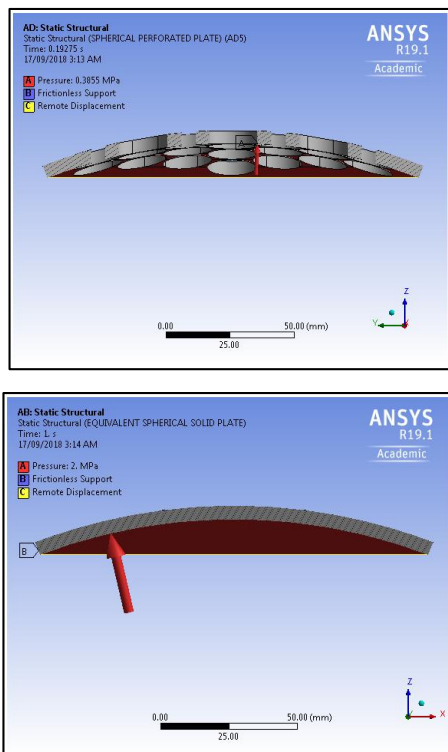


Figure 7: Spherical perforated plate and equivalent solid plate loading and boundary condition setup.

IV. RESULTS

As mentioned earlier, the aim of this research is to extend the equivalent material properties concept to the spherical perforated plate. Flat and spherical plates with triangular perforation patterns normal to the surface were considered. Additionally, a spherical plate with perforation parallel to surface was also considered.

IV.I Flat perforated plate

FEA analysis was first carried out in order to re-assess the ASME design curve for the flat perforated plate. The effective elastic constants obtained for different ligament efficiencies were tabulated as shown in Table 1 below.

Table 1: FEA results for the equivalent material constants.

η	E^*/E	$\nu^* (\nu=0.3)$
0.05	0.015	0.815
0.1	0.048	0.673
0.2	0.145	0.490
0.3	0.275	0.388
0.4	0.385	0.330
0.5	0.53	0.299
0.6	0.66	0.283
0.7	0.785	0.286
0.8	0.875	0.284
0.9	0.94	0.290
1.0	1	0.30

The curves of the equivalent material properties versus the ligament efficiencies were then generated as shown in Fig 8 below.

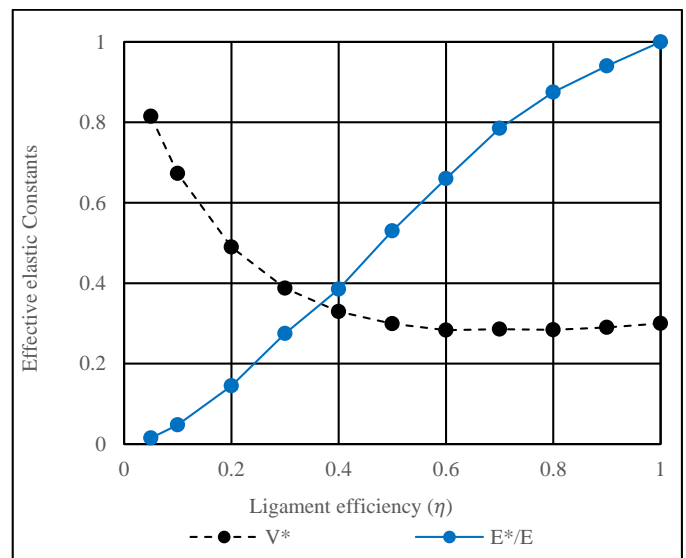


Figure 8. Equivalent material properties of the flat perforated plate

In order to verify the methodology used to determine the equivalent material properties for the flat perforated plate by FEA, the curves were compared with the design curves provided in the ASME Section III Appendix A-8000. The curves are in good agreement with the design curve. Evidence for this is shown in Fig 9 next page.

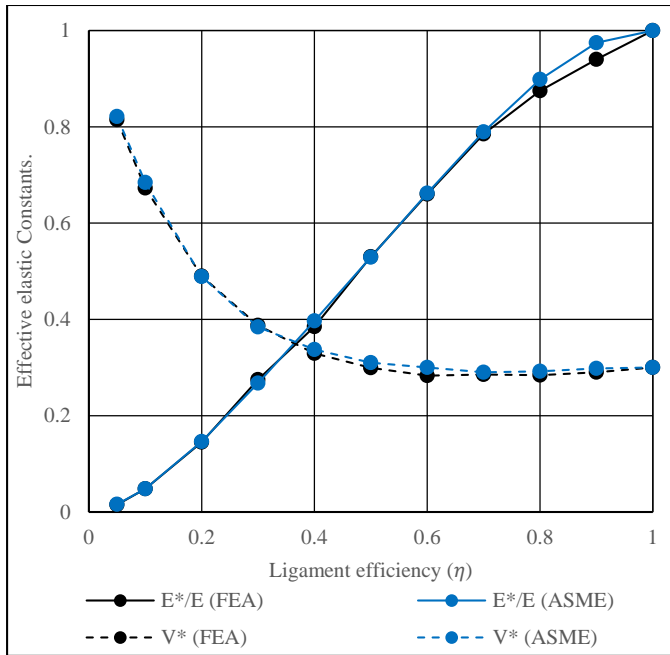


Figure 9. Comparison of FEA analysis effective elastic constants result for flat perforated plate and ASME

IV.II Spherical perforated plate

Case 1: Spherical plate with perforations parallel to the plane

The FEA methodology and the concept of equivalent material properties for a flat perforated plate was extended to the spherical perforated plate. FEA results for the equivalent elastic constants were tabulated as shown in **Error! Reference source not found.** below.

Table 2: Equivalent elastic constants

η	E^*/E	ν^* ($\nu=0.3$)
0.05	0.015	0.738
0.1	0.048	0.603
0.2	0.145	0.423
0.3	0.275	0.329
0.4	0.385	0.288
0.5	0.53	0.261
0.6	0.66	0.255
0.7	0.785	0.270
0.8	0.875	0.287
0.9	0.94	0.296
1.0	1	0.30

The curves of the equivalent material properties versus the ligament efficiencies were then generated as shown in Fig 10 below.

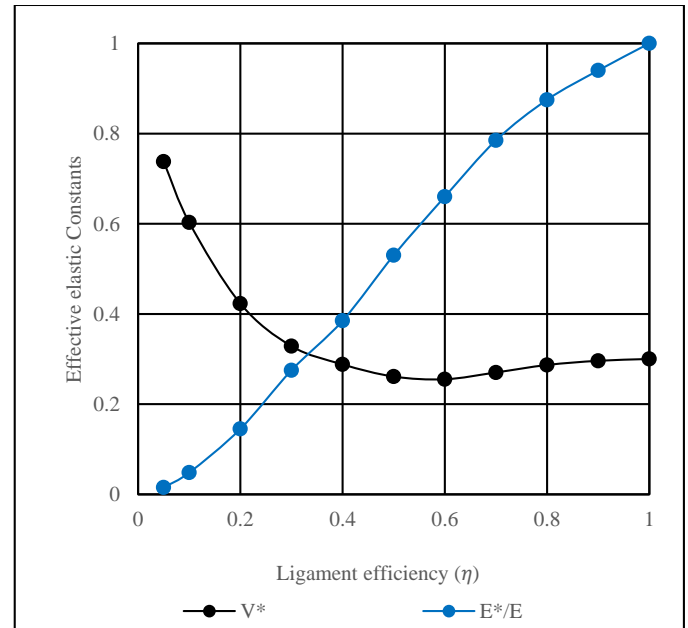


Figure 10. Equivalent elastic constants for a spherical plate with perforation parallel to the plane.

Case 2: Spherical plate with perforations normal to the surface.

The results for the spherical plate with perforation out of the plane was tabulated as shown in Table 3 below.

Table 3: Equivalent elastic constants

η	E^*/E	ν^* ($\nu=0.3$)
0.05	0.015	0.738
0.1	0.048	0.603
0.2	0.145	0.432
0.3	0.275	0.329
0.4	0.385	0.288
0.5	0.53	0.261
0.6	0.66	0.252
0.7	0.785	0.243
0.8	0.875	0.261
0.9	0.94	0.274
1.0	1	0.30

The curves of the equivalent material properties versus the ligament efficiencies were then generated as shown in Fig 11 below

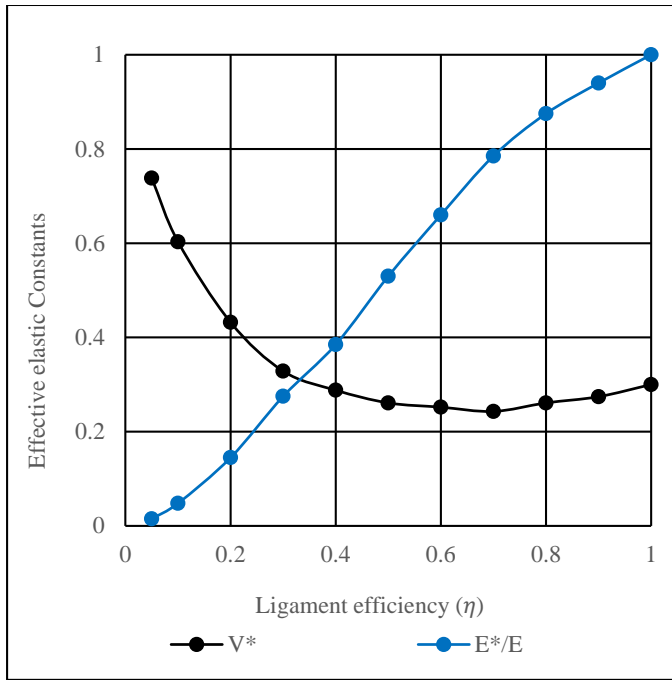


Figure 11. Equivalent elastic constants for a spherical plate with perforation normal to the surface

The curves of the equivalent material properties of the spherical perforated plate with perforation normal to the surface and parallel to the plane were compared as shown in Fig 12 below

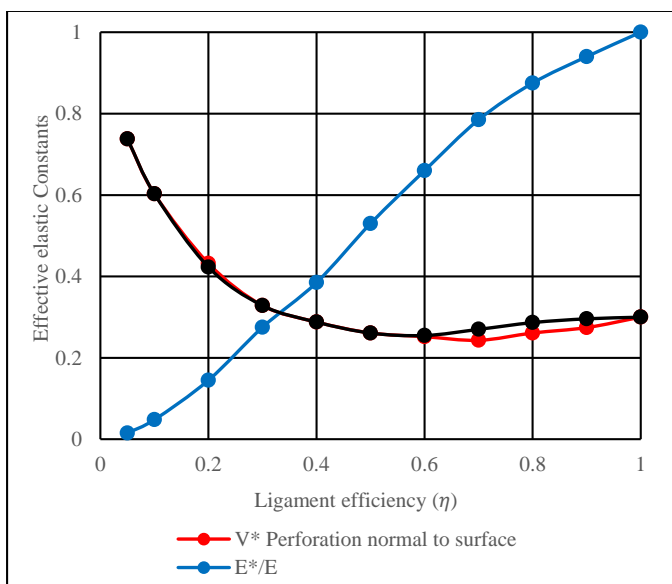


Figure 12. Comparison of the equivalent material properties of the spherical plate with perforation normal to the surface and parallel to the plane.

The curves of the flat and spherical plates for both cases i.e. with perforation normal to the surface and parallel to the plane were compared as shown in Fig 13 below.

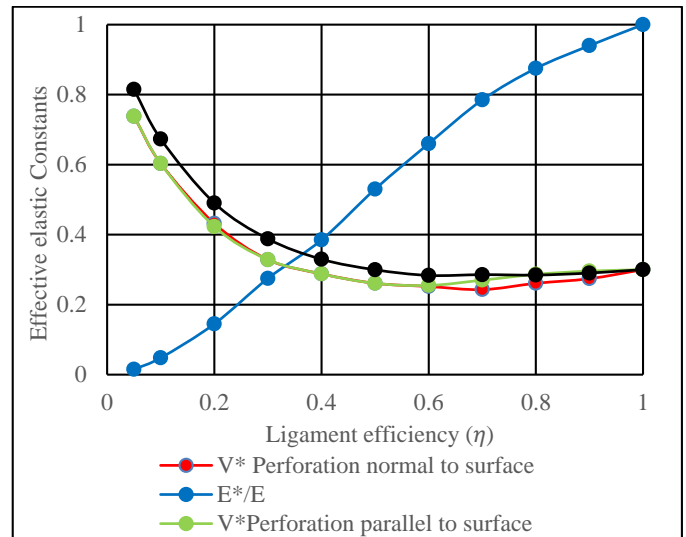


Figure 13. Comparison of the equivalent material properties of the flat plate and spherical plate with perforation normal to the surface and parallel to the plane.

V. DISCUSSIONS AND CONCLUSIONS

ASME Section III Appendix A-8000, states the methodology for the design and analysis of perforated plates. However, the methodology is limited to the flat perforated plate. In this study, the equivalent material properties concept is extended to the spherical perforated plate using FEA analysis.

FEA methodology was developed to determine the equivalent material properties. To validate the methodology, the curves generated from equivalent material properties of the flat perforated plates were compared to the design curve provided by ASME codes. The curves were in good agreement as expected but not precise due to the degree of mesh refinement of the plates. Hence, for more accurate results fine mesh is required in the vicinity of the perforations which in turn more time is required to carry out the analysis.

The trend of curves of the equivalent material properties versus the ligament efficiency for the spherical perforated plate is similar to that of the flat perforated plate although it's lower. This is due to the fact that the deformation of the spherical plate is less compared to a flat plate subjected to the same loading condition.

The equivalent material properties of spherical plate with perforation normal to the surface and parallel to the plane are similar. This indicates that the orientation of the perforation does not have significant effect on the equivalent material properties. Hence, the same design curve can be used for spherical plate with perforation normal to the surface and parallel to the plane.

The results from the FEA analysis prove that the equivalent material properties can be used in the design and analysis of the spherical perforated plate with perforations normal to and out

of the plane. However, some limitations are worth noting. Modeling of the perforated plates and construction of fine meshing is quite complex and analysis require more time. Additionally, to determine the equivalent material properties several optimizations have to carry out. Future work should, therefore, include an experimental analysis to verify the equivalent material properties for a spherical perforated plate.

Acknowledgements

The authors would like to express their appreciation to KEPCO International Nuclear Graduate School (KINGS) for the support towards the successful completion of this project research.

REFERENCES

- [1] ASME Boiler and Pressure Vessel Code, "Section III, Division 1, Appendix A-8000, Stresses in Perforated Flat Plates," ASME, New York, 2010.
- [2] H. R. Bailey R, "The behavior of Perforated Plates under Plane Stress," Journal of Mechanical Engineering Science, vol. 2, no. 2, 1960.
- [3] H. R. Bailey R., "The behavior of Perforated Plates under Plane Stress," J. Mech. Eng. Sci.2, pp. 143-165, 1960.
- [4] W. O. T. Slot, "Effective Elastic Constants for Thick Perforated Plates with Square and Triangular Penetration Patterns," Journal of Engineering for Industry, pp. 935-942, 1971.
- [5] U. R. Duncan J.P, "Equivalent Elastic Properties of Perforated Bars and Plates," Journal Of Mechanical Engineering Science, vol. 5, no. 1, 1963.
- [6] M. P., "Plate with a Doubly-Periodic Pattern of Circular Holes Loaded in Plane Stress or in Bending," ASME Publication on First International Conference on Pressure Vessel Technology, 1969.